

**Picosecond Laser Source with
Single Knob Adjustable Pulse Width**

Reprint from *Proceedings of Lasers for RF Guns*, May 14–15, 1994 Anaheim, CA

Picosecond Laser Source with Single Knob Adjustable Pulse Width

R. P. Scott, C. V. Bennett, and B. H. Kolner

Electrical Engineering Department
University of California, Los Angeles
405 Hilgard Avenue
Los Angeles, CA 90024-1594

Phone: (310)825-8899 FAX: (310)206-8495 email: scott@ee.ucla.edu

ABSTRACT

We describe and demonstrate a system which can be used with many types of actively modelocked lasers to create a source of variable width picosecond pulses. This system is an active compression scheme which incorporates a resonant electro-optic quadratic phase modulator to impart the linear frequency chirp on an optical pulse. To demonstrate, we used the modulator to chirp the 85 ps pulses from a modelocked Nd:YAG laser and subsequently compressed them with a dispersive delay line to less than 6 ps. It is possible with this system to smoothly vary the pulse width from the initial width to the fully compressed width buy changing only the RF drive power going to the phase modulator.

It has come to our attention that the ever increasing demands and requirements on lasers used in RF photoinjectors has exceeded much of the currently available technology. Ongoing research of beam dynamics in high gradient accelerators, including studies on ultra-high brightness beam transport and emittance evolution, compensation, and maintenance, have led to strict requirements on optical pulse characteristics. Amplitude stability, peak energy, timing jitter, and pulse length tailoring are just some of the parameters of interest. Presently, there are many sources of short optical pulses available commercially. Unfortunately, most of these sources do not provide low timing jitter or much flexibility in their output pulse width due to cost or technological limitations. In order to overcome the pulse width deficiency, many groups have relied on pulse compression. In general, compression is obtained by first creating a frequency sweep (linear chirp or quadratic phase modulation) across the optical pulse and then using a linear dispersive delay of the proper sign to compress the pulse (remove the chirp).

Generation of the additional frequencies required to chirp the pulse generally necessitates the use of nonlinear optical processes. The most common technique is self phase modulation (SPM) which occurs simply by passing a pulse through an optical Kerr medium. When an intense optical pulse is passed through a nonlinear medium, the refractive index, n , is altered by the optical electric field, E . This can be expressed as $n = n_0 + n_2 \langle E^2 \rangle + \dots$, where n_0 is the linear index, n_2 is the second order nonlinear index, and $\langle E^2 \rangle$ is the time average (w.r.t. carrier) of the squared electric field (i.e. \propto intensity). The variation in refractive index results in a change in phase, $\Delta\varphi$, given by

$$\Delta\varphi = n_2 \langle E^2 \rangle \frac{\omega_o z}{c}, \quad (1)$$

where ω_o = optical frequency, c = speed of light, and z = distance traveled in the Kerr medium. Since instantaneous frequency is equal to the first time derivative of phase, the frequency sweep is given by

$$\Delta\omega = \frac{n_2 \omega_o z}{c} \frac{d}{dt} \langle E^2(t) \rangle. \quad (2)$$

This frequency sweep can then be removed by a dispersive delay, such as a diffraction grating pair, set to the value required for proper compression (cancellation of chirp).

Optical fibers are the most common Kerr media used in pulse compression¹ since they confine the optical power to a small, well defined region which allows large intensities to be achieved with relatively low power. But, the fiber generates undesired nonlinear effects if peak powers exceed more than a few hundred watts. Also, because of the nature of SPM, undesired higher order modulation is present in the pulse as it exits the fiber. This can be a problem since it can not be compensated by means of linear dispersive delay lines. Most significantly, fiber-grating compression is a noisy process by nature. If there are any fluctuations in the pulse envelope, whether in its width or peak power, they will considerably change those same characteristics of the compressed pulse. Finally, since the amount of chirp imparted on the pulse is determined by the pulse envelope, the useful power range for a desired pulse width is quite narrow.

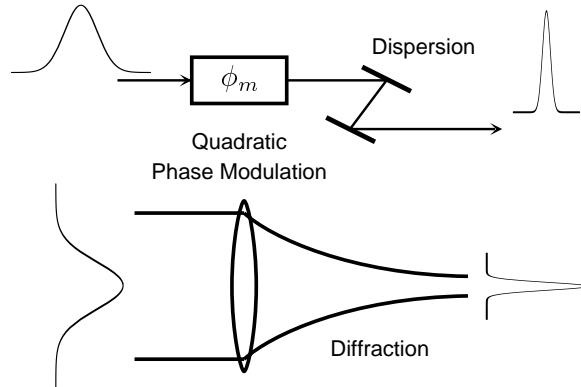


Figure 1. Optical pulse compression as the temporal analog of focusing a beam. The role of the spatial lens is played by the quadratic phase modulator, ϕ_m , and free-space diffraction is replaced by dispersion (diffraction grating pair).

Fortunately, there is a much better way of obtaining pulse compression. It is related to the theory of temporal imaging first described by Kolner and Nazarathy². They show that temporal quadratic phase modulation (imparting linear chirp) is entirely equivalent to the behavior of a thin lens on a beam in space (see Figure 1). With this in mind, we can now look at any process which provides a temporal quadratic phase modulation as a time lens and, like its spatial counterpart, a time lens can be configured to temporally “focus” the pulse³. This was demonstrated years ago using electro-optic modulators in conjunction with dispersive delay lines formed from resonant atomic vapor^{1,4–6}. Later this was demonstrated by Kolner using a traveling wave electro-optic phase modulator and diffraction gratings and was designated active pulse compression⁷.

In order to understand this approach we need to go back to the basic theory of how an electro-optic modulator (EOM) operates. The EOM works on the Pockels effect, which produces a change in the index of refraction that is linear in an applied external field. Therefore, if a sinusoidal field is applied along the material, there will be regions of no index change (nodes) and regions of maximum index change (cusps). It is the cusp regions that are of greatest interest, for if we apply a Taylor series expansion we find that the electric field variation near the maxima is quadratic. This leads to a quadratic change in the index. Thus, if the electric field is propagating within the material, as with

a traveling RF field, then any optical pulse which is copropagating within a cusp will experience a quadratic phase change (linear chirp)⁸. The amount of phase modulation is dependent on many factors including: strength of electric field, strength of electro-optic coefficient, and the total interaction length. Another important factor is the phase matching between the optical group velocity and the RF phase velocity. If these are not exactly matched then the optical pulse will exhibit “walkoff”. In other words, the pulse will slip away from the RF cusp as they propagate through the media causing higher order phase modulation in the pulse. These notions can be expressed in the following form⁸

$$\Gamma(\xi, \tau) = \Gamma_o \frac{\sin\left(\frac{\Delta\phi}{2}\right)}{\left(\frac{\Delta\phi}{2}\right)} \cos\left(\frac{\Delta\phi}{2} + \omega_m\tau + \theta\right), \quad (3)$$

where $\Gamma(\xi, \tau)$ is the net phase retardation (modulation), ξ is the propagation distance, τ is the local time variable, Γ_o is the peak phase deviation in the absence of velocity walkoff, ω_m is the microwave frequency, θ is an initial offset, and $\Delta\phi = \omega_m\xi(1/v_{go} - 1/v_{pm})$ is the phase offset due to velocity mismatch between the optical group and microwave phase velocities respectively. Several factors influencing the net modulation are grouped together in the Γ_o term of Eq. (3) which is defined as

$$\Gamma_o = \frac{\omega_o\Delta n_o\xi}{c} \quad (4)$$

where c is the speed of light and Δn_o is the peak index change for the applied peak electric field and the particular electro-optic coefficients. The amount of frequency chirp that is imparted on the pulse is related to the net phase deviation and modulation frequency by

$$\frac{d\omega}{dt} = \Gamma(\xi, \tau)\omega_m^2. \quad (5)$$

As Eqs. (3)–(5) indicate, one of the most significant aspects of this type of pulse compression is the phase modulation’s independence from optical pulse power. Therefore, unlike the fiber-grating case, the relative amplitude noise of the optical pulse is not modified when compressed. Also, these equations show how the active pulse compression

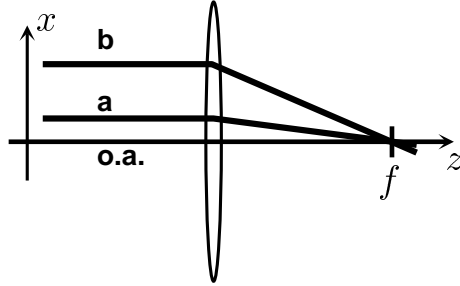


Figure 2. Effect of transverse beam jitter at the focal point (f). The transverse jitter before the lens becomes angular jitter at the focus.

scheme may be used with only a single knob to adjust the pulse width. That knob is the RF drive power going to the modulator.

Another important element of active pulse compression is the reduction of timing jitter⁹. To understand this, let's look at the spatial analogy of active pulse compression. In the absence of aberrations, if a beam of light (a) parallel to the optic axis is incident on a convex thin lens as in Figure 2, it will pass through the optic axis at the focal point (f) of the lens. Now, if the beam is offset (b) from the optic axis it will still pass through focal point although at some slightly different angle (spatial frequency). Thus, if the beam has jitter transverse to the direction of propagation it will not have any spatial jitter at the focal point. In this case, the spatial jitter has been transformed to angular (frequency) jitter. Now, from the space-time analogy, the transverse variable, x , in the spatial domain corresponds to the local time variable, τ , in the temporal domain⁸. And similar to the spatial case, any timing jitter in the pulse at the input of the compression system will be reduced to zero at the output (temporal focal point). Of course this only holds true if the system is aberration free and the dispersion is set to exactly cancel the phase modulation of the time lens. This behavior does not exist in fiber-grating (passive) pulse compression.

As in the spatial case, there are certain criteria which must be satisfied in order obtain an essentially aberration free system. The most basic criterion results from the assumption that an optical pulse acquires quadratic phase modulation if it propagates

under a cusp of the microwave electric field. This has been shown to be true⁷ if the input pulse width is less than $\approx T/6$ where T is the period of the microwave field. If the input pulse width exceeds this value, higher order terms of the sinusoidal expansion become significant and linear dispersive delays will not completely compensate the phase. The spatial analogy to this is spherical aberration. This occurs when the paraxial condition is not satisfied and rays pass through portions of the lens which are not solely quadratic and they acquire higher order phase modulation resulting in a larger spot at the focus. References [7, 9, 10] show the effects of overfilling the time lens (RF cusp) on both the envelope and the timing jitter of the pulse.

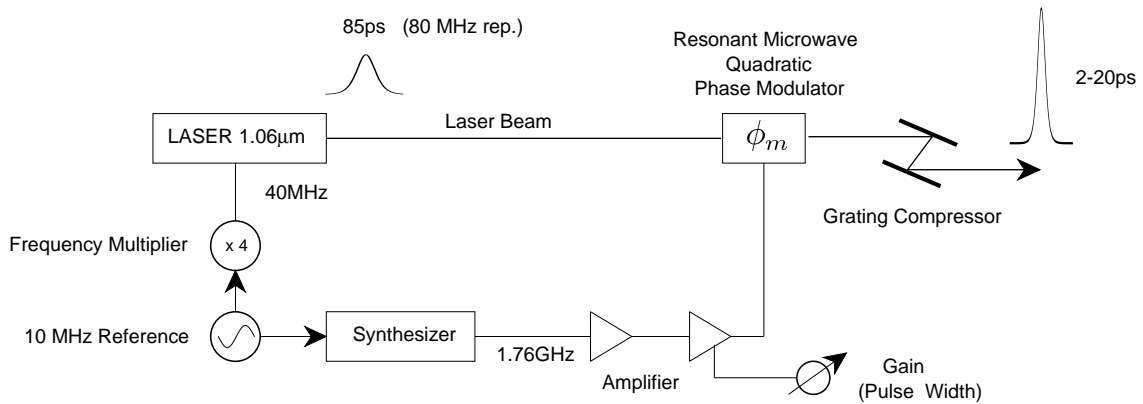


Figure 3. Schematic diagram of the the basic active compression scheme showing the origin of the RF drive power and variability of the pulse width.

So far, we have only discussed modulators of a traveling wave design. Unfortunately, for our purposes, these do not offer a very efficient use of the microwave power. This can be avoided by using a microwave resonant structure, thus increasing the electric field strength for a given microwave input power. Although simple in principle, the design is a challenge due to the many constraints required for use as an optical phase modulator. In order to demonstrate a practical active pulse compressor we designed and fabricated a time lens based on a microwave resonant structure which would compress the pulses originating from our modelocked Nd:YAG laser (80 MHz rep. rate). A schematic diagram of the active compression system is shown in Figure 3. The basis of the initial

RF resonator design was from the early work of Kaminow¹¹ and is cast in the form of a partially loaded dielectric ridge waveguide. We chose lithium niobate, LiNbO_3 , as the electro-optic crystal for several reasons. It has a large electro-optic coefficient, high optical transmission, low RF loss, good thermal conductivity, large RF and optical power limits, and it is readily available in reasonable sizes at reasonable costs. The RF drive frequency we used was 1.76 GHz. Many factors come into consideration when making this choice. First, it is a harmonic (22nd) of the laser's repetition rate. Second, the RF period is $> 6 \times \tau_p$ where τ_p is the laser pulse width, 85 ps (FWHM). This insured the phase modulation would be quadratic. Finally, the drive frequency in combination with the resonator and crystal geometry, determined how well the RF phase velocity was matched to the optical group velocity and was important in minimizing single pass walkoff.

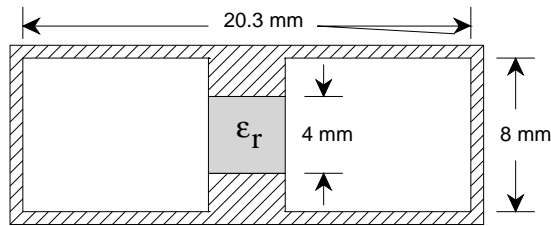


Figure 4. Cross section of dielectric loaded ridge waveguide resonator. The crystal is 40 mm long and the resonator supports a TE_{101} mode at 1.76 GHz with a loaded $Q = 1470$.

A cross section of the resonant phase modulator is shown in Figure 4. It is closed in on each end except for small apertures which give optical access to the crystal. The resonator supports a TE_{101} mode at the design frequency of 1.76 GHz and the crystal is 40 mm in length. The resonator design was fine tuned using Hewlett-Packard's High Frequency Structure Simulator (HFSS) program which uses finite element analysis to model electromagnetic fields in arbitrary geometries. This was necessary in order to account for the changes in resonant frequency due to the insertion of the coupling probe and tuning dielectric.

In order to maximize the phase modulation we obtained from our modulator, we inserted it into a hemispherical optical multi-pass cavity as shown in Figure 5. The

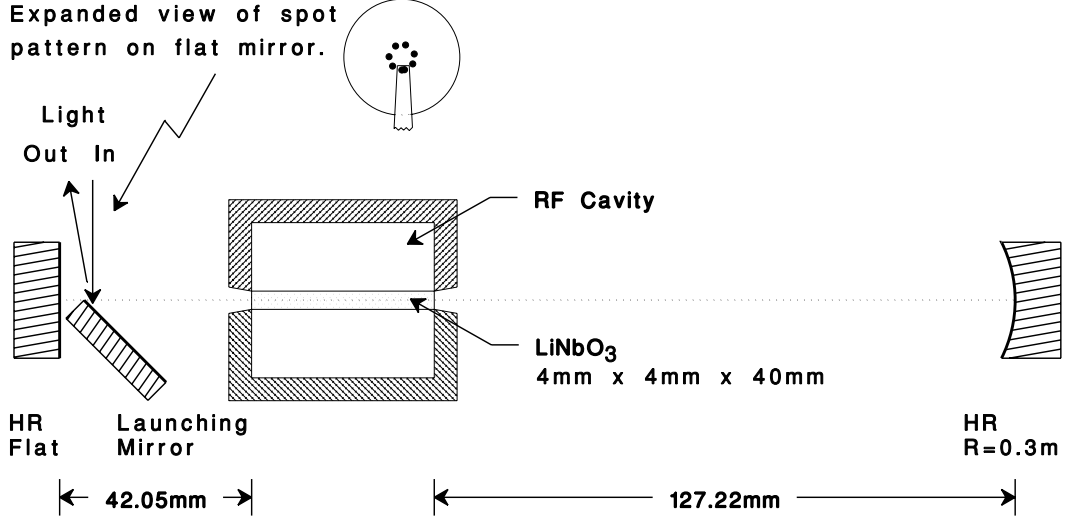


Figure 5. Resonant phase modulator placed in an optical cavity of hemispherical design. The seven spot pattern on the face of the flat mirror indicates a total of 14 passes. The separation between the flat mirror and the left crystal face is $\approx T/4$ and the separation between the curved mirror and right crystal face is $\approx 3T/4$.

optical cavity design seems straightforward in principle but, the numerous constraints involved while using it with a quadratic phase modulator make this a challenge. Two of the major concerns are timing of the RF and optical pulse, and maximizing the number of passes through the modulator. The initial timing of the optical pulse under a cusp of the RF traveling wave is set by adjusting an RF delay line. The optical multi-pass cavity must maintain the proper timing of the pulse and RF from pass to pass, compensating for single pass walkoff in the crystal and the 180° RF phase shift at the ends of the resonator. For a TE_{10m} microwave resonator in an optical cavity, the minimum single pass optical delay is $(m + 1)T/2$ and the minimum separation between an end mirror and the closest crystal face is

$$d_{min} = \frac{1}{2} \left[\left(\frac{m+1}{2} \right) cT - n\ell \right], \quad (6)$$

where n is the index of refraction of the crystal and ℓ is the length of the crystal. Any extra single pass delay, Δd , between an end mirror and its closest crystal face must correspond to integer multiples, N , of one-half RF periods (i.e. $\Delta d = NcT/2$).

The mirror curvature and position were chosen by the following factors: optical cavity

stability, spot size at input/output mirror, spot size in the crystal (important at high peak power), spot size at the crystal faces (avoid clipping), and the desired number of passes through the crystal^{12,13}. It should be noted that when optimizing the design of a multipass EOM the choice of crystal dimensions should include the tradeoff between a large cross section and shorter length (many passes) and a smaller cross section and longer length (higher electric field).

To characterize the modulator we used a Helium-Neon laser as a single pass probe. This yielded a modulation efficiency of 1 radian/ $\sqrt{\text{Watt}}$ at $\lambda = 0.633 \mu\text{m}$ (recall electro-optic modulation goes as the square root of the driving power). For our wavelength of $1.064 \mu\text{m}$ the efficiency should be $1 \times 0.633/1.064 = 0.595$ radian/ $\sqrt{\text{Watt}}$ (single pass). For the 14 pass configuration we expect a modulation efficiency of 8.33 radian/ $\sqrt{\text{Watt}}$. From this and the expression for the optimum pulse compression ratio of a gaussian pulse⁷, below, we can calculate the compressed pulse width, τ_o , for a given drive power.

$$\frac{\tau_i}{\tau_o} = \sqrt{1 + [(\Gamma_o \pi^2 / \ln 2)(\tau_i/T)^2]^2} \quad (7)$$

In our case we used a maximum RF drive power of 32 Watts. Therefore, the expected compression ratio was 15:1 and the expected compressed pulse width was 5.7 ps.

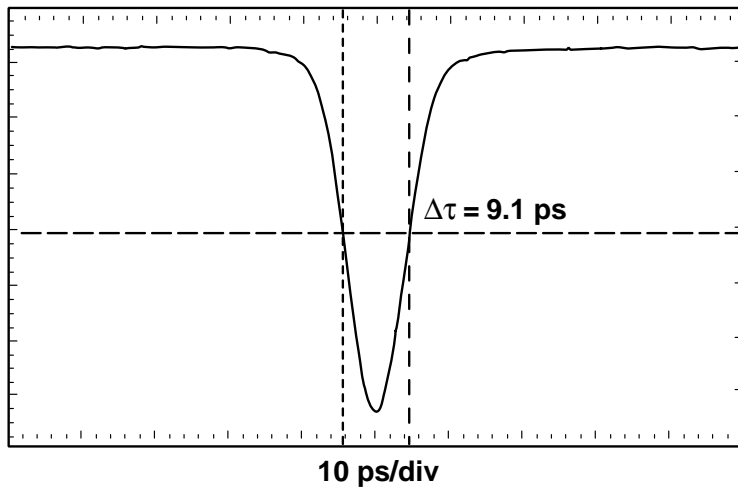


Figure 6. Autocorrelation trace of a pulse compressed with the active pulse compression setup shown in Figs. 3-5. Notice the complete absence of a pedestal or wings indicating nearly uniform linear chirp.

Figure 6 shows a typical compressed pulse (no averaging) when the RF drive power was at its maximum (32 Watts). The pulse is clean and free from a pedestal (or wings) normally seen with fiber-grating compressors. The measured autocorrelation width is 9.1 ps. This implies that the true pulse width is 5.9 ps, if a sech^2 pulse shape is assumed. Since the input pulse from the laser was 85 ps, this gives a compression ratio of 14.4:1.

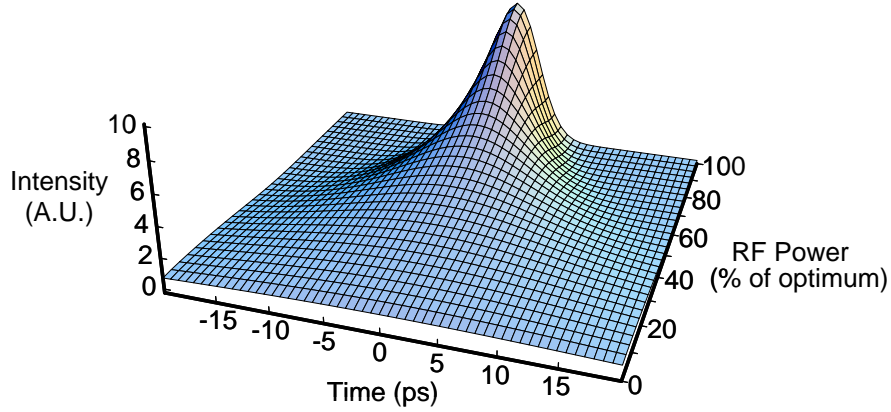


Figure 7. Theoretical example showing how a variation in RF drive power effects the output pulse of an active compression system. For this case f_{RF} is 2.856 GHz, τ_i is 58.3 ps, and Γ_o is 25 radians @ 100% RF power.

Figure 7 demonstrates how the pulse characteristics will theoretically vary with changing RF power when a configuration similar to the one shown in Figure 3 is used. In this instance, the dispersion (grating pair) has been optimized for minimum pulse width at the maximum RF power that produces $\Gamma_o = 25$ radians. The RF drive frequency is 2.856 GHz and the input pulse width is 58.4 ps ($T/6$). With no RF power, the pulse is broadened by the dispersion to 58.7 ps (although this is not visible in the plot). As the power is increased to 100% the pulse compresses to a minimum of 5.9 ps. This yields a compression ratio of $\sim 10:1$.

Another way of viewing how the active pulse compressor operates as a variable pulse width source is shown in Figure 8. The performance of the compressor can be optimized for a given value of Γ_o by adjusting the dispersion to cancel the imparted chirp. The maximum compression ratio is shown by curve (e) and is a plot of Eq. (7) with $f_{\text{RF}} = 1/T = 2.856$ GHz and the input pulse width, $\tau_i = 58.3$ ps. Curves (a-d) are plots of the

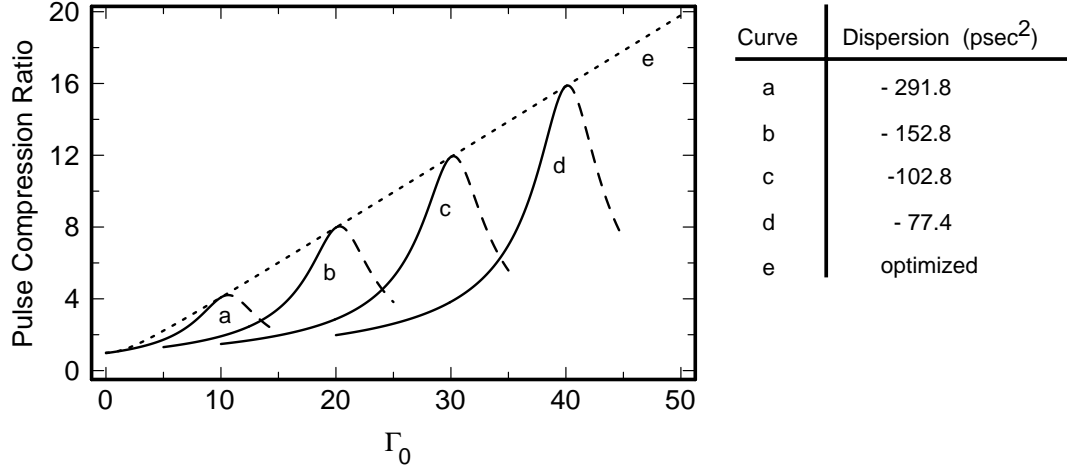


Figure 8. Theoretical plot of pulse compression ratio showing the dependence on peak phase deviation, Γ_o . Curves (a-d) represent the compression ratio as function of Γ_o and *fixed* values of dispersion. Curve (e) is the optimum compression ratio for Γ_o and is described by Eq. (7). The drive frequency, f_{RF} , is 2.856 GHz, and the input pulse width, τ_i , is 58.3 ps.

compression ratio for varying peak phase deviation ($\propto \sqrt{\text{RF Power}}$) and a *fixed* value of dispersion. Notice that the compression ratio increases steadily from $\Gamma_o = 0$ to the peak but, begins to decrease if you exceed the optimum compression point for a curve (i.e. increase Γ_o beyond the optimum value of fixed dispersion).

In summary, there are three areas where active pulse compressors can make significant contributions to RF photocathode development. The most obvious, is the ease by which the optical pulse widths may be varied. Once configured for optimum compression, reducing the RF drive power to the electro-optic time lens will broaden the output pulse from the active compression system. Replacement of optical components or realignment of the system is unnecessary. Systems currently using fiber-grating pulse compression will notice a great improvement in pulse to pulse amplitude stability by switching to an active pulse compressor. Unlike fiber-grating compressors, input pulse amplitude noise has no effect on the pulse compression of an active compression system. Finally, for those systems which require small amounts of timing jitter, active pulse compression will reduce, and in some cases eliminate, timing jitter from the pulse.

The authors would like to acknowledge support from the National Science Foundation (NSF# ECS 9110678), the Advanced Thermionics Research Initiative (ATRI) program, and the David and Lucile Packard Foundation.

REFERENCES

1. D. Grischkowsky, *Appl. Phys. Lett.*, vol. 25, pp. 566-568, 1974.
2. B. H. Kolner and M. Nazarathy, *Opt. Lett.*, vol. 14, pp. 630-632, 1989.
3. B. H. Kolner, C. V. Bennett, and R. P. Scott, *Proc. SPIE OE/LASE*, vol. 2116, paper #37, 1994.
4. J. A. Giordmaine, M. A. Duguay, and J. W. Hansen, *IEEE J. Quant. Elect.*, vol. QE-4, pp. 252-255, 1968.
5. J. E. Bjorkholm, E. H. Turner, and D. B. Pearson, *Appl. Phys. Lett.*, vol. 26, pp. 564-566, 1975.
6. J. K. Wigmore and D. R. Grischkowsky, *IEEE J. Quant. Elect.*, vol. QE-14, pp. 310-315, 1978.
7. B. H. Kolner, *Appl. Phys. Lett.*, vol. 52, pp. 1122-1124, 1988.
8. B. H. Kolner, *IEEE J. Quant. Elect.*, To be published Aug. 1994.
9. M. T. Kauffman, A. A. Godil, B. A. Auld, W. C. Banyai, and D. M. Bloom, *Electron. Lett.*, vol. 29, pp. 268-269, 1993.
10. A. A. Godil, B. A. Auld, and D. M. Bloom, *Appl. Phys. Lett.*, vol. 62, pp. 1047-1049, 1992.
11. I. P. Kaminow and W. M. Sharpless, *Appl. Optics*, vol. 6, pp. 351-352, 1967.
12. W. R. Trutna and R. L. Byer, *Appl. Optics*, vol. 19, pp. 301-312, 1980.
13. A. E. Siegman, *Lasers*, University Science Books, Mill Valley, CA, 1986.